

# Hybrid Effective Thermal Conductivity Expression on the Composite and Porous Structures

Murat Tekelioğlu

Department of Mechanical Engineering, Karabük University, Karabük 78050, Turkey  
tekelioglu@karabuk.edu.tr

**Abstract:** Knowledge of thermal properties of those structures that incorporate large cavities or materials with different thermal properties is essential to the quantification of the amount of heat transfer through these structures. For example, it is important to be able to quantify  $\kappa_{eff}$  (effective thermal conductivity) on the porous and composite structures. In this work, a substrate material incorporating many large cavities, or incorporating many materials with different  $\kappa$  values, was focused on. Here, the cavity sections (or materials with different  $\kappa$  values) and substrate sections had average widths of about 2.493mm and 2.431mm, respectively. A mathematical expression was derived for  $\kappa_{eff}$  in 1D taking into account the total numbers and widths of each cavity and substrate section. In the presented hybrid mathematical expression of  $\kappa_{eff}$ ,  $\kappa_{eff}$  expressions given earlier of the series and parallel arrangements were put together. Available expressions for the series arrangement, parallel arrangement, and Maxwell-Eucken 1 (ME1) formulation were compared with the acquired hybrid  $\kappa_{eff}$  value.  $\varepsilon$  (porosity) values of  $\varepsilon = 14.67\%$ ,  $\varepsilon = 34.91\%$ ,  $\varepsilon = 48.57\%$ , and  $\varepsilon = 65.91\%$  were selected for comparison purposes. The total numbers and size distributions of the cavity and substrate sections must be known in priori.

**Keywords:** Composite material, porous material, substrate, thermal conductivity

## 1. INTRODUCTION

There has been numerous work in the literature related to the structures incorporating small and micro-size cavities. For example, both thermal conductivities and thermal diffusivities of the samples coated at different substrate rotation speeds were shown to decrease with an increase of temperature from the room temperature to 1,000°C [1]. Porous Si (PS) layer thermal conductivity was presented with the thickness of the PS layer [2]. In the other work, thermal conductivity and temperature profiles were studied on the micro porous layers [3].

In the available literature,  $\kappa_{eff}$  derivations were included.  $\kappa_{eff}$  ( $W \cdot m^{-1} \cdot K^{-1}$ ) indicated the overall thermal conductivity of a material after taking into account the different thermal conductivities of different material parts. These available expressions in the literature included only series and parallel arrangements and a hybrid expression (a mixture of the series and parallel arrangements) has not been cited.

In the present paper, a hybrid  $\kappa_{eff}$  expression (combination of the series and parallel arrangements  $\kappa_{eff}$ ) was derived after taking into account the size, distribution, and total number information of the cavity and substrate sections.

## 2. ANALYSIS

In order to begin with the present analysis, total numbers of the cavity and substrate sections were selected. Thus, total numbers of 7 cavities and 8 substrates were taken. The numbers corresponded to a total structural length ( $L$ ) of 36.9mm. A structure with  $L = 50mm$  could also be investigated. Size of each cavity and substrate section and total numbers of the cavity and substrate sections were quantified in random manner. It was aimed to establish irregular (unidentical) widths for the cavity and substrate sections.

In thermal problems involving  $\kappa_{eff}$ , validity of the “Classical Mechanics” method is set by the Knudsen number ( $Kn$ ).  $Kn$  was calculated to verify the applicability of the current approach. Both time and length scales can be considered in using  $Kn$  on structures. Specifically, the radiative thin ( $Kn \gg 1$ ) and radiative thick ( $Kn \ll 1$ ) limits are defined. In the present work,  $\kappa_c$  (cavity section

thermal conductivity) and  $\kappa_s$  (substrate section thermal conductivity) values were calculated separately. After this, each material slice (strip) was expressed according to the series arrangement and the series arrangement results were put together according to the parallel arrangement to give the hybrid  $\kappa_{eff}$  value of the entire structure.

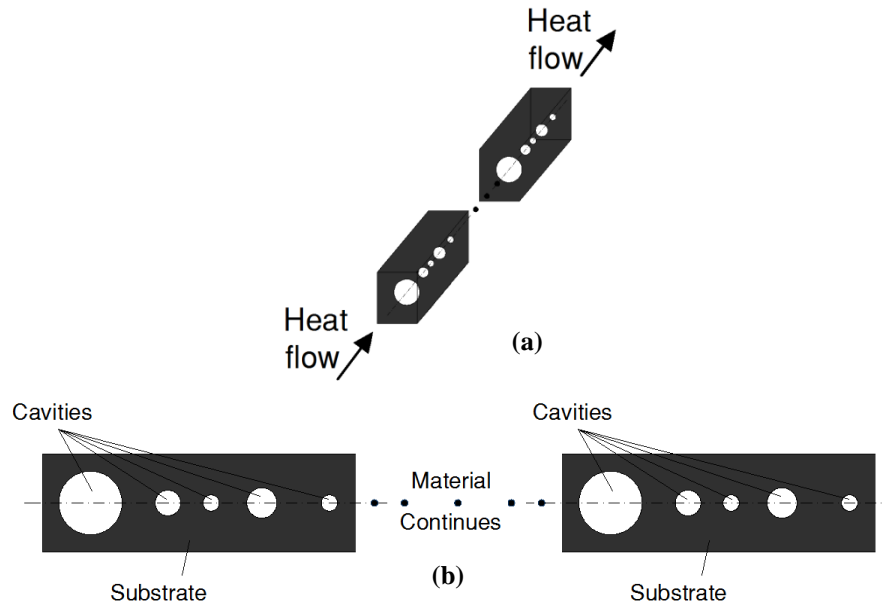


**Figure 1.** Cavity and substrate sections shown with arbitrary size and sequence. a) Isometric view. b) Frontal view.

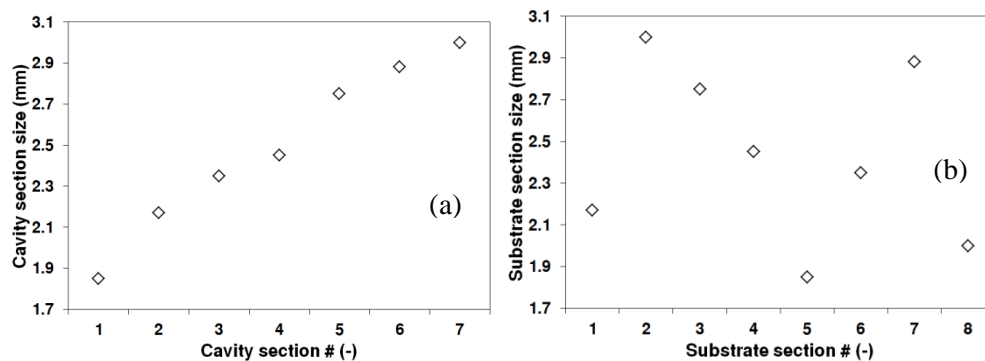


**Figure 2.** Sample size distribution ( $L = 36.9\text{mm}$ ): a) Total cavity section size ( $L_c = 17.45\text{mm}$ ). b) Total substrate section size ( $L_s = 19.45\text{mm}$ ).

This study focused on the Silica-type non-crystalline material with the prespecified total numbers of the cavity and substrate sections inside. The structure considered in this study may also be a composite one in which case the cavity sections may be replaced with materials of different  $\kappa$  ( $\kappa_c$ ) values embedded inside the substrate material. The cavities were taken as empty cubic spaces. In practice, volumetric space of a cavity holds a random shape. Also, volumetric space of each cavity section can be thought of as a perfect sphere distributed randomly throughout the substrate (Figure 1). Figure 2 shows the size distributions about the studied cavity and substrate sections. Thermal conductivity of the thermal insulators was given [6]

$$\kappa_s = \frac{1}{3} \rho c_v v_a \Lambda_{ph} \quad (1)$$

where  $\rho c_v$  is the lattice volumetric specific heat ( $J \cdot m^{-3} \cdot K^{-1}$ ),  $v_a$  is the average speed of the phonons ( $m/s$ ), and  $\Lambda_{ph}$  is the phonon mean free path,  $\Lambda_{ph} = v_a \tau$  ( $m$ ). Thin-film Silica properties including  $\kappa_s$  and  $\Lambda_s$  were extensively evaluated in [4]. For a solid rod with a thickness much smaller than the thermal radiation wavelength, the speed of sound ( $v_a$ ) was given by the expression  $v_a = \sqrt{E/\rho}$ . Here,  $E$  is the Young's modulus of the material ( $E = 3\text{GPa}$  for vitreous glass) and  $\rho$  is the density ( $\rho = 1,000\text{ kg} \cdot m^{-3}$  for vitreous glass). Some polymers were reported to show non-crystalline glass behavior in the literature [5]. Also, most glasses are accepted to possess amorphous

non-crystalline structures. It was stated in [6] that  $\kappa$  values of the crystalline materials are usually higher than that of the non-crystalline materials owing to their lattice vibrations. Brick Silica fused thermal properties were used on the substrate material.

Thermal conductivity of the cavities filled up with air was given in [4]

$$\kappa_c = \frac{\kappa_{c,free}}{1+2\cdot\beta\frac{\Lambda_c}{t_p}} \quad (2)$$

where  $\kappa_{c,free}$  is the thermal conductivity of the cavity filled up with free air ( $W \cdot m^{-1} \cdot K^{-1}$ ),  $\Lambda_c$  is the mean free path of the gas molecules at atmospheric pressure ( $\Lambda_c = \frac{k_B T}{\sqrt{2} \cdot \sigma_0 \cdot P}$ ),  $t_p$  is the characteristic size of the cavity filled up with air ( $m$ ),  $\beta$  is a constant ( $\beta = \frac{5\pi}{32} \cdot \frac{2-\alpha}{\alpha} \cdot \frac{9\gamma-5}{\gamma+1}$ ),  $\gamma = 1.4$  (for air), and  $\alpha = 1$  (for air). There are certain pressure and temperature dependencies of  $\kappa_{c,free}$  as well as of  $\kappa_s$  as stated in [4]. That is,  $\kappa_c$  and  $\kappa_s$  change somewhat as a function of pressure and temperature. This change is attributed to the fact that  $\Lambda_c$  (and  $\Lambda_s$ ) vary with temperature [4]. In [4],  $\kappa_{eff}$  of the entire Silica structure was shown to have a substantially lower value than  $\kappa_{c,free}$  with pressure of the confined gas inside the cavity.

As  $Kn$  increased, this was shown to decrease the value of  $\kappa_{eff}$  on thin films, thin wires, or rods [6]. Also, for a Silicon substrate, impurities present inside the substrate were noted to decrease the value of  $\kappa_s$  [6]. This fact makes such nano and micro porous structures invaluable materials in providing effective insulation. Arrangements of the cavity and substrate sections are shown in Figure 3. An insulation material (for example, a building insulation material) is usually subjected to different temperatures at both of its surfaces. Constant and uniform temperatures,  $T_1 = cst$  and  $T_2 = cst$ , were assumed at both surfaces of the insulation material, as was illustrated in Figure 3.

For a porous material,  $\varepsilon$  is not precise and is usually an estimate. In the present study, the cavity size distribution, total number, and sequence (order) are required; the information related to the size distribution, total number, and order of the substrate sections must also be available in priori. When a material structure is in the hybrid arrangement of Figure 3(c), a mathematical expression of  $\kappa_{eff}$  is sought.  $\kappa_{eff}$  of a composite structure or of a structure with irregular large pores was represented.

$\kappa_{eff}$  can readily be given from the literature for the series arrangement of the substrate and cavity sections (Figure 3(a)) as

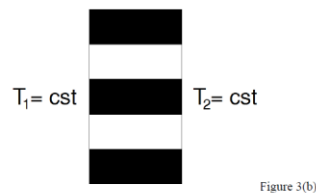


**Figure 3.** Cavity and substrate sections: a) Series arrangement. b) Parallel arrangement. c) Hybrid arrangement (combination of the series and parallel arrangements). Hybrid arrangement was shown for demonstration and consisted of four cavity and five substrate sections. Dark shades are the substrate sections and white regions are the cavities or materials of different  $\kappa$  values.

$$\kappa_{eff} = \frac{1}{\frac{\varepsilon}{\kappa_c} + \frac{1-\varepsilon}{\kappa_s}} \quad (3)$$

and as

$$\kappa_{eff} = \varepsilon\kappa_c + (1 - \varepsilon)\kappa_s \quad (4)$$

for the parallel arrangement of the substrate and cavity sections shown in Figure 3(b). In Eqs. (3) and (4),  $\varepsilon$  is the ratio of the cavity volume to the total structural volume, or  $\varepsilon = V_c / (V_c + V_s)$ . Although these expressions call for somewhat macro porosities, they have been implemented on the micro structures with some extent giving an idea about the magnitude of  $\kappa_{eff}$ . In [7],  $\kappa_{eff}$  formulations of the series arrangement (Eq. (3)) and parallel arrangement (Eq. (4)) were swapped. There are further simplifications to  $\kappa_{eff}$  in the literature. For example, if the ratio of the thermal conductivities of the substrate and cavity sections is about one order of magnitude or higher, then  $\kappa_{eff}$  was included [7], or other exponential expressions were defined [7]. In some instances, the theoretical expressions of [7] were just qualitative assessments of the experimental results giving optimistically at least about 1.469 times higher results.

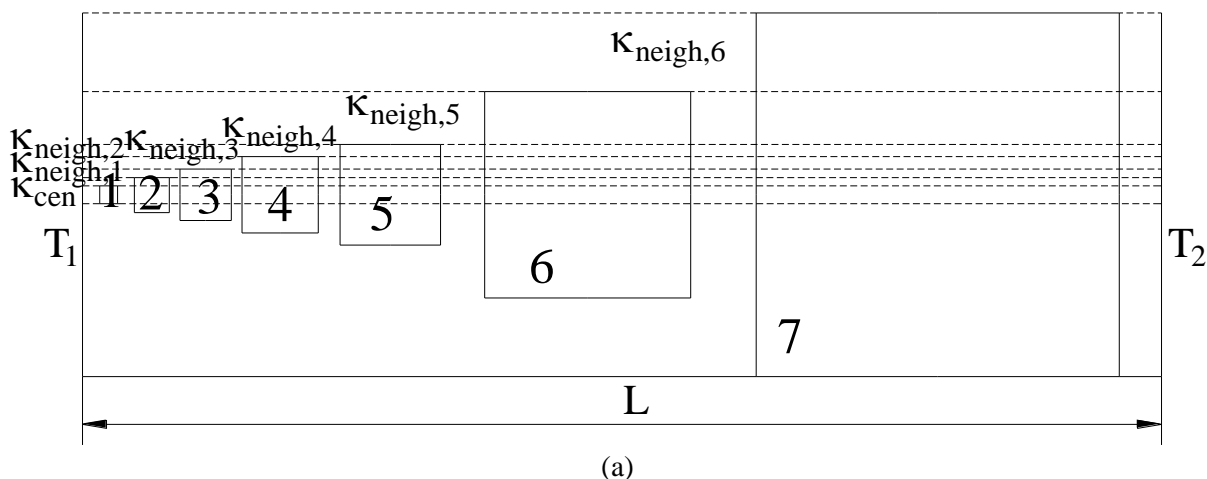
Inclusion of the Silica particles of 10nm-size inside a Silica grain network porous structure was reported [7] to decrease the  $\kappa$  value significantly ( $\kappa = 0.030 W \cdot m^{-1} \cdot K^{-1}$ ) at atmospheric pressure. Thus, such porous structures were shown to have better insulation capabilities. Heat transfer and flow characteristics were analyzed on the micrometer-size channels incorporating  $\varepsilon$  ([8] and [9]). Ultrahigh convective heat transfer enhancement was reported on the surfaces of the nano porous layers [10]. Textbooks have included extensive outline of composite structures including approach methodology [11-13]. For example, Torquato[13] discussed using micro modeling within an RVE (representative volume element). In [12], a brief mention of overall thermal measures for microscopically heterogeneous media is given.

A comparison between the present mathematical derivation (hybrid arrangement of the series and parallel arrangements of Figure 3(c)) was made with the results of the Maxwell-Eucken 1 (ME1) formulation [7]. The Maxwell-Eucken 1 (ME1) formulation was thus far the best formulation to make these comparisons against. Based on this formulation, when continuous phase is the substrate and dispersed phase is the cavity,  $\kappa_{eff}$  was represented with

$$\kappa_{eff} = \kappa_s \frac{2\kappa_s + \kappa_c - 2(\kappa_s - \kappa_c)\varepsilon}{2\kappa_s + \kappa_c + (\kappa_s - \kappa_c)\varepsilon} \tag{5}$$

In [7], it was also shown that  $(\kappa_{eff} / \kappa_s)$  of a random porous structure will be somewhere in between the series and parallel arrangement  $(\kappa_{eff} / \kappa_s)$  values: Parallel arrangement setting the upper limit and the series arrangement setting the lower limit. The formulation in Eq. (5) was noted to be valid for small porosity values ( $\varepsilon \lesssim 0.25$ ). The substrate-cavity arrangement as a 1D problem of the Maxwell-Eucken 1 (ME1) formulation is a quite close approximation of the present substrate-cavity system of Figure 3(c). The Maxwell-Eucken 1 (ME1) formulation result was compared with the presently calculated hybrid  $\kappa_{eff}$  value. In the Maxwell-Eucken 1 (ME1) formulation, total numbers and size distributions of the cavity and substrate sections are not known, thus, not substituted. A comparison made with the Maxwell-Eucken 1 (ME1) formulation is only likely when  $\varepsilon$  is known or measured. A better comparison of the present model results may be established with the experiments. Methods for acquiring  $\kappa_{eff}$  of porous materials were described in [7], however, for structures incorporating large cavities, or for structures incorporating composites, a hybrid  $\kappa_{eff}$  is needed.

Most appropriate methods in acquiring  $\kappa_c$  of air ([6] and [4]) and  $\kappa_s$  Silica-type materials [6] are described.



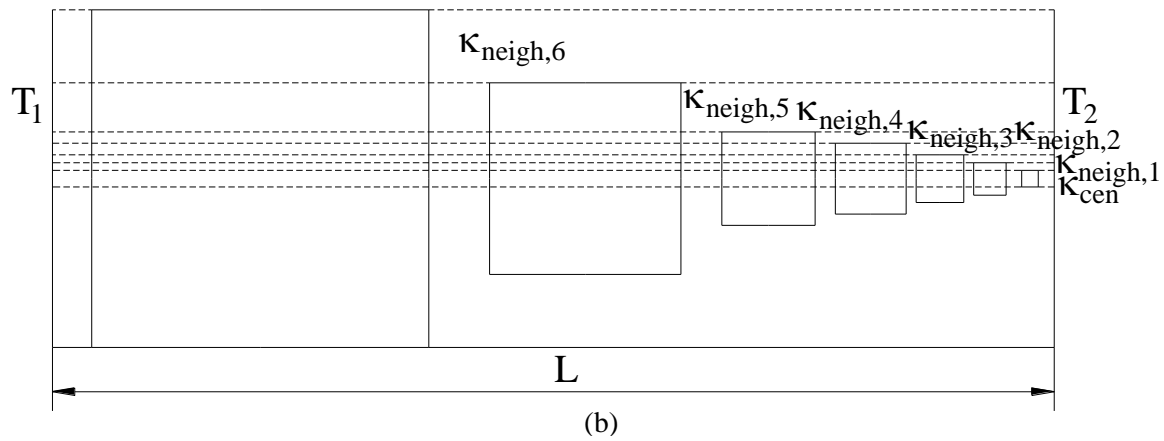


**Figure 4.** Cavity and substrate sections from the high temperature end toward the low temperature end: a) In ascending order, b) In descending order. A total of 7 and 8 cavity and substrate sections were demonstrated, respectively. Each cavity was approximated as a cubic space filled up with air. These cavities may also represent materials with different  $\kappa$  values. ( $L = 36.9\text{mm}$ ).

In the analysis, slices of independent cavity and substrate sections were taken and the hybrid  $\kappa_{eff}$  expression was written. Although the present hybrid  $\kappa_{eff}$  expression was derived based on heat transfer in 1D, the heat transfer is, in fact, a 2D process on the planar geometry and a 3D process on the volumetric geometry incorporating also the heat transfer between other neighboring slices. Thus, the amount of heat transfer in 2D or 3D is less than the amount of heat transfer in 1D. This is because of the fact that that is heat transferred in the extra dimensions. The heat transfer process or  $\kappa_{eff}$  in 2D or 3D was not focused in this work.

Figure 4 illustrates the hybrid arrangement of the cavity and substrate sections. A total of 7 cavity sections were taken embedded inside 8 Silica substrate sections. These 7 cavity and 8 substrate sections can also be sequenced in any other random order.  $\kappa_{eff}$  was defined on the slices of the parallel arrangements of the cavity and substrate sections (See Figure 3(b) and Figure (4)) in transverse direction for which each substrate (Silica) section was represented by  $\kappa_s$  and each cavity section by  $\kappa_c$ .

Considering Figure 3(c) and Figure (4), we first write the local effective thermal conductivity on the center-line ( $\kappa_{cen}$ ) after starting from the smallest cavity (near to the higher temperature surface,  $T_1$ ) and going toward the largest cavity (near to the lower temperature surface,  $T_2$ ). Already written on the center-line, this  $\kappa_{cen}$  expression was taken and repeated after decreasing the cavity number by 1 each time a slice is shifted in the transverse direction likening it to the series arrangement of the cavity and substrate sections (Figure 3(a)). On the center-line,

$$\kappa_{cen} = \left[ \frac{1}{\sum_{i=1}^{n+1} \frac{d_{s,i}}{\kappa_s \cdot A_{s,cen}} + \sum_{i=1}^n \frac{d_{c,i}}{\kappa_c \cdot A_{c,cen}}} \right] \cdot \frac{L}{A_{cen}} \quad (6)$$

where  $A_{cen} = A_{s,cen} = A_{c,cen} = d_{c,1} \cdot d_{c,1}$  and  $L$  is the total length of the material. On the neighboring area in transverse direction, the heat transfer surface area until next cavity section is reached changes and  $\kappa_{neigh,m}$  becomes

$$\kappa_{neigh,m} = \left[ \frac{1}{\frac{1}{\kappa_s \cdot A_{s,m}} (\sum_{j=1}^{m+1} d_{s,j} + \sum_{j=1}^m d_{c,j}) + \sum_{i=m+2}^{n+1} \frac{d_{s,i}}{2\kappa_s \cdot A_{s,m}} + \sum_{i=m+1}^n \frac{d_{c,i}}{\kappa_c \cdot A_{c,m}}} \right] \cdot \frac{L}{A_{neigh,m}} \quad (7)$$

where *neigh* means neighboring and  $m$  is the number of the neighboring slice (for example,  $m = 1$  for the first neighboring slice in the transverse direction and  $m = 1, \dots, n - 1$ ),  $A_{neigh,m} = A_{s,m} = A_{c,m} = (d_{c,m+1} \cdot d_{c,m+1} - d_{c,m} \cdot d_{c,m})$ . Thus, total number of the cavities determines the magnitude of  $m$ . Next,  $\kappa_{cen}$  of Eq. (6) and  $\kappa_{neigh,m}$  of Eq. (7) are assembled according to the parallel arrangement of Figure 3(b) so that  $\kappa_{eff}$  could be calculated.  $\kappa_{eff}$  was calculated with the following

$$\kappa_{eff} = \frac{\kappa_{cen} \cdot A_{cen} + \sum_{m=1}^{n-1} \kappa_{neigh,m} \cdot A_{neigh,m}}{A} \quad (8)$$

where  $A = (\text{largest cavity dimension}) \cdot (\text{largest cavity dimension})$ . As it was illustrated in Figure 4, when the sequence of the cavity and substrate sections are switched (a large cavity switches its position with a small cavity), calculated  $\kappa_{eff}$  changes and needs a recalculation. Eq. (8) evaluates  $\kappa_{eff}$  value for a material taking into account the total numbers and statistical distributions of the cavity and substrate sections. The slice method that was used in the derivation of Eq. (8) has the identical assumptions made in the derivations of the series and parallel arrangement effective thermal conductivity expressions in the literature (See Figure 3(a) and Figure 3(b)). Each slice is in resemblance of the parallel arrangement of Figure 3(b).

The present mathematical expression (Eq. (8)) was compared against other available models, for example, against Maxwell-Eucken 1 (ME1) formulation (Eq. (5)), and series (Figure 3(a)) and parallel (Figure 3(b)) arrangements of the cavity and substrate sections. Maxwell-Eucken 1 (ME1) formulation of Eq. (5) does not include any information related to the total numbers and sizes of the cavity or substrate sections. Macro-size cavity calculations with the present formulation (Eq. (8)) derived based on the geometry in Figure 3(c)) makes the difference between the series and parallel arrangement  $\kappa_{eff}$  values more visible.

### 3. RESULTS AND DISCUSSION

The results of the present study from Eq. (8) were shown in Figure 5.  $\kappa_{eff}$  values can clearly be identified in Figure 5. Eq. (8) represented a hybrid expression of the effective thermal conductivity combining series and parallel arrangements of the cavity and substrate sections. The discrepancy between the Maxwell-Eucken 1 (ME1) formulation [7] and the present study was also identified. In presentation of  $\kappa_{eff}$ , such effects as the boundary scattering between a cavity section and a substrate section may be influential. It is important to point out that Maxwell-Eucken 1 (ME1) formulation does not include information about the total numbers or statistical sizes of the cavity and substrate sections inside the structure and assumes that the cavities are scattered quite randomly throughout the substrate. Hence, to some extent, in terms of the total number and size information of the cavity and substrate sections, Maxwell-Eucken 1 (ME1) formulation is unspecific. On the contrary, usually it is hard to obtain precise numbers for the total number of cavities when they are small. The comparisons were established for the radiative thick ( $Kn \ll 1$ ) and micro-to-macro size structures where the ‘‘Classical Mechanics’’ formulations were still applicable.  $\kappa_s$  and  $\kappa_c$  values can be calculated from the ‘‘Quantum Mechanics’’ [6].  $\kappa_{eff}$  expression calculated with Eqs. (6-8) can also be implemented on structures supporting large numbers of cavities (for example, structures with  $n = 500,000$  cavity sections and  $n + 1 = 500,001$  substrate sections).

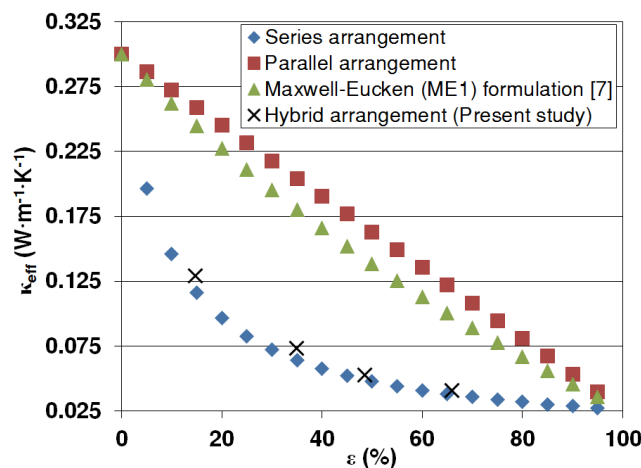


**Figure 5.** Series arrangement, parallel arrangement, hybrid arrangement (present study, Eq. (8), Figure 4(a)), and Maxwell-Eucken 1 (ME1) formulation (Eq. (5)) [7].  $\kappa_c = 0.026 W \cdot m^{-1} \cdot K^{-1}$ ,  $\kappa_s = 0.300 W \cdot m^{-1} \cdot K^{-1}$  (Brick, Silica fired).  $\epsilon = 14.67\%$ ,  $\epsilon = 34.91\%$ ,  $\epsilon = 48.57\%$ , and  $\epsilon = 65.91\%$ .

### 4. CONCLUSIONS

Aim of this study was to derive a hybrid effective thermal conductivity expression following the series and parallel arrangements of the cavity and substrate sections. This hybrid arrangement expression resulted in a  $\kappa_{eff}$  value somewhat between the series and parallel arrangements being



closer to the series arrangement result. Present hybrid  $\kappa_{eff}$  expression may be equally applicable to the composite structures and porous structures. Size, distribution, and total number information are required of the cavity and substrate sections. Experimental and numerical simulations are necessary to validate the current results. The hybrid method is more suited to structures with small number of cavities.

#### REFERENCES

- [1] Jang, B.K., and Matsubara, H., 2006, Influence of porosity on thermo physical properties of nano-porous zirconia coatings grown by electron beam-physical vapor deposition, *Scripta Materialia*, 54, 1655–1659.
- [2] Lysenko, V., Périchon, S., Remaki, B., Barbier, D., 2002, Thermal isolation in microsystems with porous silicon, *Sensors and Actuators A-Physical*, 99, 13-24.
- [3] Burheim, O.S., Su, H., Pasupathi, S., Pharoah, J.G., Pollet, B.G., 2013, Thermal conductivity and temperature profiles of the micro porous layers used for the polymer electrolyte membrane fuel cell, *International Journal of Hydrogen Energy*, 38, 8437-8447.
- [4] Coquard, R., Baillis, D., Grigorova, V., Enguehard, F., Quenard, D., Levitz, P., 2013, Modelling of the conductive heat transfer through nano-structured porous silica materials, *Journal of Non-Crystalline Solids*, 363, 103–115.
- [5] N. Brun, P. Bourson, S. Margueron, M. Duc, “Study of the thermal behavior of syndiotactic and atactic polystyrene by raman spectroscopy”, in *AIP Proc. of The 14th International Esaform Conference on Material Forming: Esaform 1353*, 2011, p. 856.
- [6] Z. M. Zhang, *Nano/Microscale Heat Transfer*, New York, United States: McGraw-Hill, 2007, p. 175, p. 164, p. 175.
- [7] Yuan, J., and Sundén, B., 2013, On continuum models for heat transfer in micro/nano-scale porous structures relevant for fuel cells, *International Journal of Heat and Mass Transfer*, 58, 441–456.
- [8] Wan, Z.M., Liu, J., Su, K.L., Hu, X.H., M, S.S., 2011, Flow and heat transfer in porous micro heat sink for thermal management of high power leds, *Microelectronics Journal*, 42, 632–637.
- [9] Shokouhmand, H., Isfahani, A.H.M., Shirani, E., 2010, Friction and heat transfer coefficient in micro and nano channels filled with porous media for wide range of knudsen number, *International Communications in Heat and Mass Transfer*, 37, 890–894.
- [10] Kunugi, T., Muko, K., Shibahara, M., 2004, Ultrahigh heat transfer enhancement using nano-porous layer, *Super lattices and Microstructures*, 35, 531–542.
- [11] G. W. Milton, *The Theory of Composites*, Cambridge, United Kingdom: Cambridge University Press, 2002.
- [12] S. Nemat-Nasser, and M. Hori, *Micro mechanics: Overall Properties of Heterogeneous Materials*, 2nd ed., New York, United States: North Holland, 1998.
- [13] S. Torquato, *Random Heterogeneous Materials: Microstructure and Macroscopic Properties*, New York, United States: Springer, 2002.

#### AUTHOR'S BIOGRAPHY



**Murat Tekelioğlu** is currently an Assistant Professor of Mechanical Engineering in the Karabük University. He received his B.Sc. Degree in Mechanical Engineering from the İstanbul Technical University, Turkey, in 1998. He received his M.Sc. and Ph.D. Degrees in Mechanical Engineering from the University of Nevada, Reno, U.S.A. in 2000 and 2005, respectively. His main interests include the energy, energy conversion systems, mathematical modelling, and simulation.